The Reaction of N(^{4}S) with CH_2F: A Comparative ab Initio and DFT Study

Bibiana Menéndez,[†] Víctor M. Rayón,[†] José A. Sordo,*[,†] Alvaro Cimas,[‡] Carmen Barrientos,[‡] and Antonio Largo*[,‡]

Laboratorio de Química Computacional, Departamento de Química Física y Analítica, Facultad de Química, Universidad de Oviedo, 33006, Oviedo, Spain, and Departamento de Química Física, Facultad de Ciencias, Universidad de Valladolid, 47005 Valladolid, Spain

Received: May 8, 2001; In Final Form: August 14, 2001

The triplet potential energy surface for the N(^{4}S) + $CH_2F(^2A')$ reaction has been studied employing both MP2 and DFT(B3LYP) methods. The energies of the involved species have been refined using the G2, CBS, and CCSD(T) methods, respectively. The general picture for this reaction is a typical addition−elimination mechanism, where initially a rather stable intermediate, $^{\bullet\bullet}NCH_2F$, is obtained by the interaction of nitrogen with the radical through the carbon atom. There are two preferred products from the thermodynamic viewpoint, *trans*-$FC^{\bullet}{=}NH$ and $HFC{=}N^{\bullet}$, the latter one being slightly more stable. Other possible products, such as $H_2C{=}N^{\bullet}$ and *trans*-$HC^{\bullet}{=}NH$, are also exothermic but less stable, whereas *cis*-$HC^{\bullet}{=}NF$ is even clearly endothermic. From the kinetic viewpoint, $HFC{=}N^{\bullet}$ is predicted to be the preferred product. It seems that neither isomerization nor subsequent elimination of hydrogen or fluorine atoms from the primary products is feasible, since all these processes are much less exothermic and involve considerable kinetic barriers.

Introduction

The reaction of N atoms with methyl radicals has been the subject of different theoretical[1] and experimental studies.[2,3] This reaction is of interest in several fields, such as astrochemistry (it is suggested to play an important role in the interstellar synthesis of HCN[4] and in the chemistry of the atmosphere of Titan[5]), as well as in combustion processes[6] and in the reaction between nitrogen and hydrocarbons.[7] A few experimental studies on the reactions of N atoms with halogenated alkyl radicals (such as $CHCl_2$ and CF_3) have also been published.[8,9] On the other hand, reactions of several halogenated alkyl radicals with oxygen atoms have been extensively studied. Seetula et al.[10,11] have carried out experimental studies of the kinetics of the reactions of chlorinated methyl radicals with O(^{3}P). In addition, Wang et al.[12−15] performed theoretical studies of the reactions of CH_2F, CH_2Cl, CHClF, and CH_3F with O(^{3}P). These reactions are of interest not only because of their relevance in combustion chemistry, but also due to their important role in atmospheric chemistry. One of the processes that halogenated alkanes can undergo in the upper atmosphere is photodescomposition to produce halogenated alkyl radicals. In addition, halogenated alkyl radical may be formed in the reactions of the corresponding halogenated alkanes with the hydroxyl radical. Once they are formed, halogenated alkyl radicals may take part in several processes with other species that are relatively abundant in the upper atmosphere, such as oxygen atoms.

Although the atmospheric relevance of the reactions of N atoms with halogenated alkyl radicals is surely not as important as in the case of O atoms, reactions of nitrogen atoms are certainly interesting from the general perspective of radical−radical reactions. In addition, the possible effect on the reaction mechanism of the substitution of hydrogen atoms by either fluorine or chlorine atoms is also another interesting question.

To the best of our knowledge, there is no theoretical information about the reaction of nitrogen atoms with halogenated alkyl radicals. In this paper, we provide a theoretical study of the reaction of N(^{4}S) with one of the simplest halogenated alkyl radicals, namely, $CH_2F(^2A')$, considering the different potential channels. In addition to the determination of the preferential products in this reaction, a second purpose of the present study is to compare different theoretical methods in order to assess their performance and to propose an affordable method of calculation that could be applied to other more complex related reactions.

Computational Methods

Ab initio methodologies, including second-order Møller−Plesset (MP2)[16] and Coupled-cluster with single and double excitations and a perturbative treatment of the connected triple excitations [CCSD(T)],[17] as well as density functional theory (DFT) with Becke's 3-parameter exchange funcional[18] and the correlation functional of Lee−Yang−Parr[19] (B3LYP), were employed to carry out an exhaustive exploration of the triplet potential energy surface (PES) corresponding to the reaction N(^{4}S) + $CH_2F(^2A')$. Pople and co-worker's standard 6-31G(d,p)[9] and Dunning's cc-pVXZ (X = D,T,Q)[20] correlation-consistent basis sets were used. The geometry optimizations were performed at the MP2/6-31G(d,p), MP2/cc-pVXZ (X = D, T), and B3LYP/cc-pVXZ (X = D, T) levels, and CCSD(T)/cc-pVTZ//B3LYP/cc-pVTZ single-point calculations were also accomplished in order to improve the energetic predictions. It has been shown recently[21−24] that CCSD(T) provides, in general, an excellent approach to the CCSDT level and therefore the CCSD(T)//B3LYP relative energies are expected to represent accurate theoretical predictions. Indeed, recent results by Lynch and Truhlar[25] suggest that the location of saddle points using hybrid density funcional methods followed by single-point CCSD(T) calculations represents a recipe that can be considered to have an excellent performance-to-cost ratio. Further refined

* Corresponding author.
[†] Universidad de Oviedo.
[‡] Universidad de Valladolid.

10.1021/jp011760e CCC: $20.00
Published on Web 10/04/2001

energetic predictions were obtained by using Pople and coworker's G2 theory[26] as well as by exploiting the important property of Dunning's correlation-consistent basis sets that exhibit monotonic convergence to an apparent complete basis set (CBS) limit.[24] The G2 theory, which exploits the approximate separability of the one-particle and *n*-particle expansions, has proved to render very accurate energy differences (within "chemical accuracy"),[24] while the estimate of the CBS limit at the MP2/cc-pVXZ (X = D,T,Q) level by using a combined Gaussian/exponential function[27] has a profound effect on improving the level of agreement with experiment.[28] In principle, the latter approach is expected to be less accurate (the correlation contribution is estimated only at the MP2 level with no further correction) but much cheaper, and consequently, it can represent an excellent choice for studies involving larger molecules. A CBS limit at the B3LYP/cc-pVXZ (X = D, T, Q) level was also computed (since no drastic changes in geometries were obtained in exploratory calculations when passing from cc-pVTZ to cc-pVQZ, MP2/cc-pVQZ//MP2/cc-pVTZ and B3LYP/cc-pVQZ//B3LYP/cc-pVTZ energies were employed to perform the extrapolations).

It is well-known that an important drawback commonly associated with the use of unrestricted Hartree−Fock (UHF) wave functions in open-shell calculations both at the self-consistent field and post-Hartree-Fock [MP2, DFT and CCSD-(T)] levels is the spin-contamination problem. We employed Schlegel's algorithm[29] to estimate approximate spin-projected MP2 energies corresponding to the appropriate multiplicity. It should be mentioned in this context that DFT methods based on unrestricted determinants for open-shell systems are not very prone to spin contamination, as a consequence of electron correlation being included in the single-determinantal wave function by means of the exchange-correlation functional.[30] On the other hand, Stanton[31] has shown that, even in CCSD, all spin contamination is essentially removed from the Coupled-cluster wave function.

All the structures located in the present study were interconnected by means of the intrinsic reaction coordinate (IRC) algorithm[32,33] as implemented in the GAUSSIAN 98 packages of programs[34] with which the calculations reported in this work were carried out.

Results and Discussion

The optimized geometries at different levels of theory of the reactant and possible products for the $N(^4S) + CH_2F(^2A')$ reaction are shown in Figure 1. The corresponding geometries for the intermediates on the triplet surface are collected in Figure 2, whereas those for the different transition structures are given in Figure 3. The intermediates have all their vibrational frequencies real (therefore they are true minima on the corresponding potential surface), whereas in the case of transition states we checked, they had just one imaginary frequency corresponding to the desired mode. To save space, we do not provide the vibrational frequencies at the different levels, but they are available upon request. Relative energies for the different species involved in the reaction at selected levels of theory are given in Table 1, and overall energetic profiles for the reaction $N(^4S) + CH_2F(^2A')$, as computed at the G2 and B3LYP/CBS levels, are shown in Figures 4 and 5, respectively. Each first part of Figures 4 and 5 shows the profile for the reaction up to formation of the primary products resulting from elimination of either hydrogen or fluorine atoms, whereas Figure 4b and Figure 5b correspond to the possible further evolution of these primary products. It should be mentioned that the energies reported in Figures 4 and 5 are all G2 or B3LYP/CBS

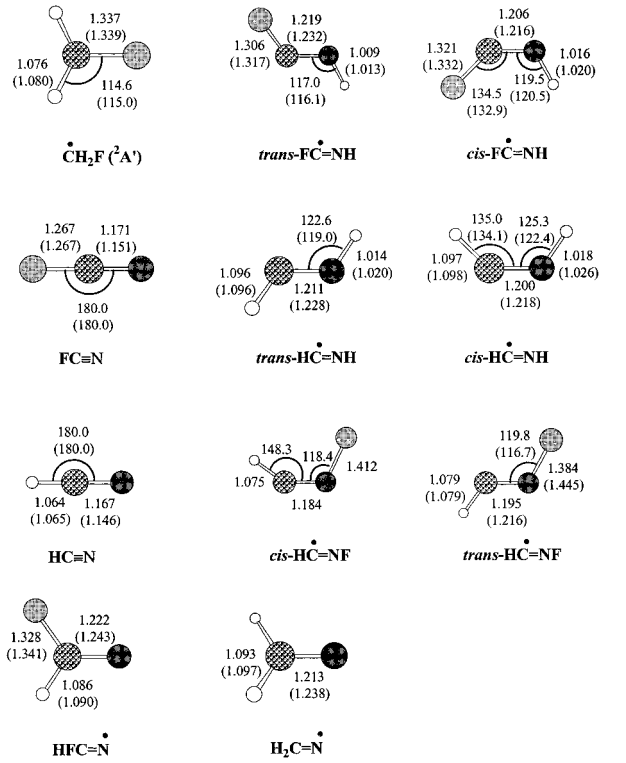

Figure 1. Most significant geometrical parameters as computed at the MP2/cc-pVTZ and B3LYP/cc-pVTZ (in parentheses) levels for the reactant and possible products of the reaction $N(^4S) + CH_2F$ ($^2A'$). Bond distances are given in Å and angles in deg.

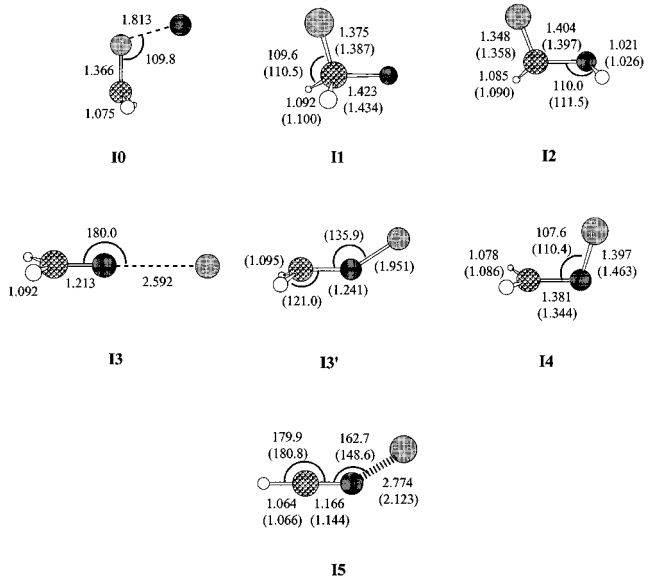

Figure 2. Most significant geometrical parameters as computed at the MP2/cc-pVTZ and B3LYP/cc-pVTZ (in parentheses) levels for the intermediates in the reaction of $N(^4S) + CH_2F$ ($^2A'$). Bond distances are given in Å and angles in deg.

values, and consequently, some apparent topological inconsistencies are present (for example, some minima become slightly lower in energy than the associated transition structures). Of course, the real (MP2-unprojected or B3LYP) PESs have been checked to be topologically consistent in all cases.

Scheme 1 shows the different channels through which the reaction between fluoromethyl radical (CH_2F; $^2A'$) and atomic nitrogen (N; ^4S) can proceed on a triplet PES. (The numbers appearing under the different reactants, products, and intermediates correspond to the G2 energies in kcal/mol. The G2 energies

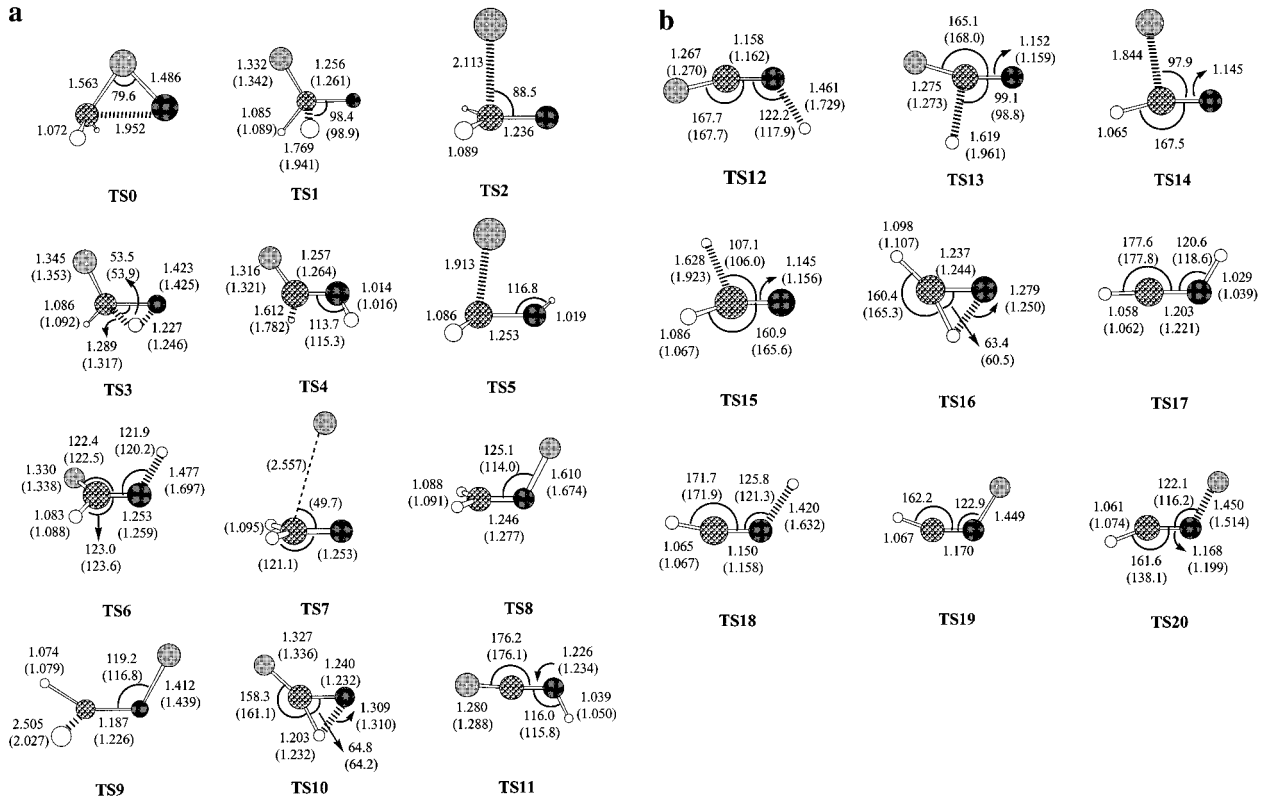

Figure 3. Most significant geometrical parameters as computed at the MP2/cc-pVTZ and B3LYP/cc-pVTZ (in parentheses) levels for the transition structures in the reaction of N(^{4}S) + CH_2F (^{2}A′). Bond distances are given in Å and angles in deg.

SCHEME 1

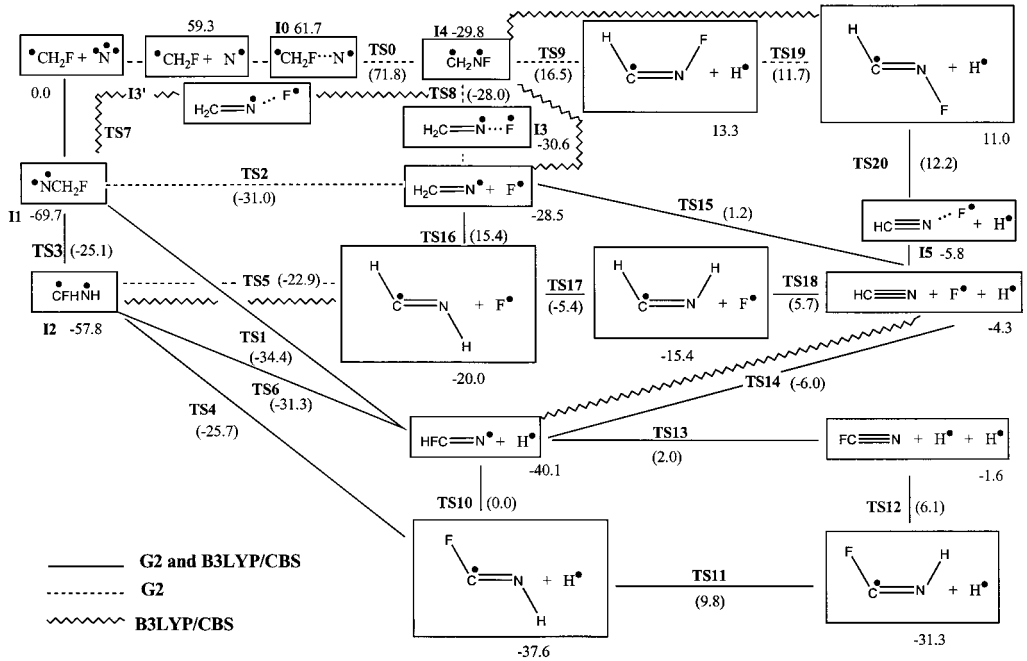

of the transition structures are given in parentheses. Since **TS7** and **I3′** were not located at the MP2 level—see discussion below—no G2 energies are available for them. Their B3LYP/CBS energies can be found in Table 1.) To provide information of chemical interest about the nature of the different structures in Scheme 1, we represented "limiting structures" taking into account the spin densities on the different atoms for each structure. Thus, for example, $^{\bullet}CH_2FN^{\bullet}$ means that the structure presents a pronounced diradical character "mainly" ascribed to the carbon and nitrogen atoms.

Inspection of the geometries computed at different levels collected in Figures 1-3 shows several trends that can be summarized as follows. The discrepancies in bond lengths and bond angles as computed with different methods (MP2, B3LYP) and basis sets [6-31G(d,p), cc-pVXZ (X = D,T)] were, in general, smaller than 0.02 Å and 3°, respectively. In the case of C−H, C−N, C═N, C≡N, and N−H bonds, the bonds lengths (R) computed at the MP2 level are R(cc-pVTZ) < R[6-31G(d,p)] < R(cc-pVDZ), whereas for the C−F and N−F bonds, the ordering is R(cc-pVTZ) < R(cc-pVDZ) < R[6-31G(d,p)].

TABLE 1: Relative Energies at Different Levels of Theory for the Different Species Involved in the Reaction of N (^{4}S) with CH_2F (^{2}A′)

	MP2						
system	6-31G(d,p)	CBS[a]	QCISD[b]	QCISD(T)[b]	G2[c]	B3LYP/CBS[b]	CCSD(T)[b]
CH_2F (^{2}A′) + N (^{4}S)	0.0	0.0	0.0	0.0	0.0	0.0	0.0
trans-FC•═NH + H•	−28.1	−42.9	−21.3	−32.1	−37.6	−40.9	−31.0
cis-FC•═NH + H•	−22.2	−36.9			−31.3	−35.0	−25.0
FC≡N + H• + H•	4.8	−12.2			−1.6	0.7	4.6
trans-HC•═NH + F•	−10.1	−19.1			−20.0	−25.1	−16.5
cis-HC•═NH + F•	−4.6	−14.6			−15.4	−21.2	−12.1
HC≡N + H• + F•	1.4	−9.3			−4.3	−3.1	−0.7
cis-HC•═NF + H•	26.3	13.0			13.3		
trans-HC•═NF + H•	25.1	12.2			11.0	5.8	17.5
HFC═N• + H•	−30.2	−41.3	−27.4	−35.2	−40.1	−42.7	−34.3
H_2C═N• + F•	−19.2	−23.8	−20.9	−26.1	−28.5	−33.0	−25.4
I0	72.4	59.1			61.7[d]		
I1	−64.8	−69.3	−59.4	−65.4	−69.7	−71.5	−64.8
I2	−49.5	−58.9	−42.3	−51.3	−57.8	−64.4	−52.1
I3 (I3′)	−19.4	−23.8			−30.6	−39.8	−24.1
I4	−20.0	−28.3			−29.8	−38.8	−24.0
I5	0.1	−4.9			−5.8		
TS0	82.4	73.6			71.8[d]		
TS1	−22.6	−34.2	−19.6	−29.2	−34.4 (−34.1)	−38.9	−28.7
TS2	−20.0	−24.7	−20.1	−26.2	−31.0 (−31.7)		
TS3	−14.2	−26.1	−9.4	−20.5	−25.1 (−24.4)	−30.9	−19.8
TS4	−9.3	−25.3	−6.5	−19.7	−25.7	−31.8	−19.1
TS5	−9.0	−19.1			−22.9		
TS6	−12.8	−29.3	−15.3	−26.1	−31.3	−38.1	−26.2
TS7						−39.4	−23.1
TS8	−10.7	−20.1			−28.0 (−28.7)	−39.3	−21.5
TS9	35.3	19.4			16.5	8.9	22.0
TS10	12.9	−6.4			0.0	−1.7	6.8
TS11	22.0	5.1			9.8	3.2	16.4
TS12	20.2	1.1			6.1	5.3	13.0
TS13	16.4	−2.2			2.0	3.6	9.8
TS14	6.1	−5.9			−6.0		
TS15	14.2	2.7			1.2	0.5	15.5
TS16	28.7	15.7			15.4	12.8	7.8
TS17	8.0	−4.3			−5.4	−11.4	−1.0
TS18	19.3	5.9			5.7	2.0	9.1
TS19	25.4	10.6			11.7		
TS20	26.7	11.4			12.2	5.1	17.7

[a] Including the ZPE correction as estimated at the MP2/cc-pVTZ level (scaled by 0.96). [b] Including the ZPE correction as estimated at the B3LYP/cc-pVTZ level. [c] G3 values in parentheses. [d] Since no HF structure was found, the ZPE correction was carried out at the MP2(FULL)/6-31G(d) level (scaled by 0.96).

Consistently, the B3LYP results show that the bond lengths estimated with cc-pVTZ are, in general, smaller than those computed with cc-pVDZ. As a general trend, the B3LYP bond lengths and angles are slightly greater than the MP2 ones for a given basis set. Particularly, the B3LYP method tends to predict looser transition structures, in agreement with Lynch and Truhlar's recent observation.[25]

Examination of the relative energies collected in Table 1 leads to the conclusion that, in general, the MP2/CBS estimates predict much more stabilized structures than the standard Pople's 6-31G(d,p) basis set. Sometimes the MP2/CBS energies are similar to those predicted by B3LYP/CBS, but in most cases, the latter ones are appreciably lower. On the other hand, the CCSD(T) method generally provides relative energies which are, for most species, quite higher than the G2 ones. Nevertheless, if relative energies are computed taking as a reference one of the intermediates instead of the reactants, the CCSD(T) values will be very close to the G2 ones, a fact already noticed in the study of another reaction involving nitrogen atoms.[35] That means that the problem with the CCSD(T) energies very probably deals with the description of N(^{4}S). This is confirmed by computation of the dissociation energy for N_2. At the G2 level, a dissociation energy of 223.83 kcal/mol is obtained, a result very close to the experimental value of 225.94 kcal/mol (incidentally, the B3LYP/cc-pVTZ method virtually matches this value, since a dissociation energy of 225.45 kcal/mol is obtained). On the other hand, the CCSD(T)/cc-pVTZ method renders a value of 212.43 kcal/mol. The apparent superiority of G2 over CCSD(T) in such cases seems to be mainly related to the so-called higher-level correction (HLC) imposed in G2 theory,[26] which introduces corrections for paired and unpaired valence electrons. The HLC correction in G2 theory for N(^{4}S) represents −0.00671 hartree (−4.2 kcal/mol). The most interesting conclusion obtained from comparison of the respective performances of the different methods is that the G2 theory predicts, in general, energy values relatively close to the MP2/CBS ones. This result suggests that the correlation contributions are reasonably well estimated at the MP2 level for the systems under study. Some exceptions to this general trend have been detected (see, for example, FC≡N in Table 1).

The reaction starts through the interaction of the carbon and nitrogen atoms, resulting in formation of an intermediate (**I1**) which takes place directly and does not involve any transition state, since both reactants are open-shell species and interact on an attractive potential surface. Since this is an important question, in Figure 6, we provide the result of the scan of the potential surface in this region at two levels of theory, namely, B3LYP/cc-pVTZ and QCISD/6-31G(d) (quadratic configuration interaction with single and double substitutions). For obtaining these figures, we have considered the approaching of the

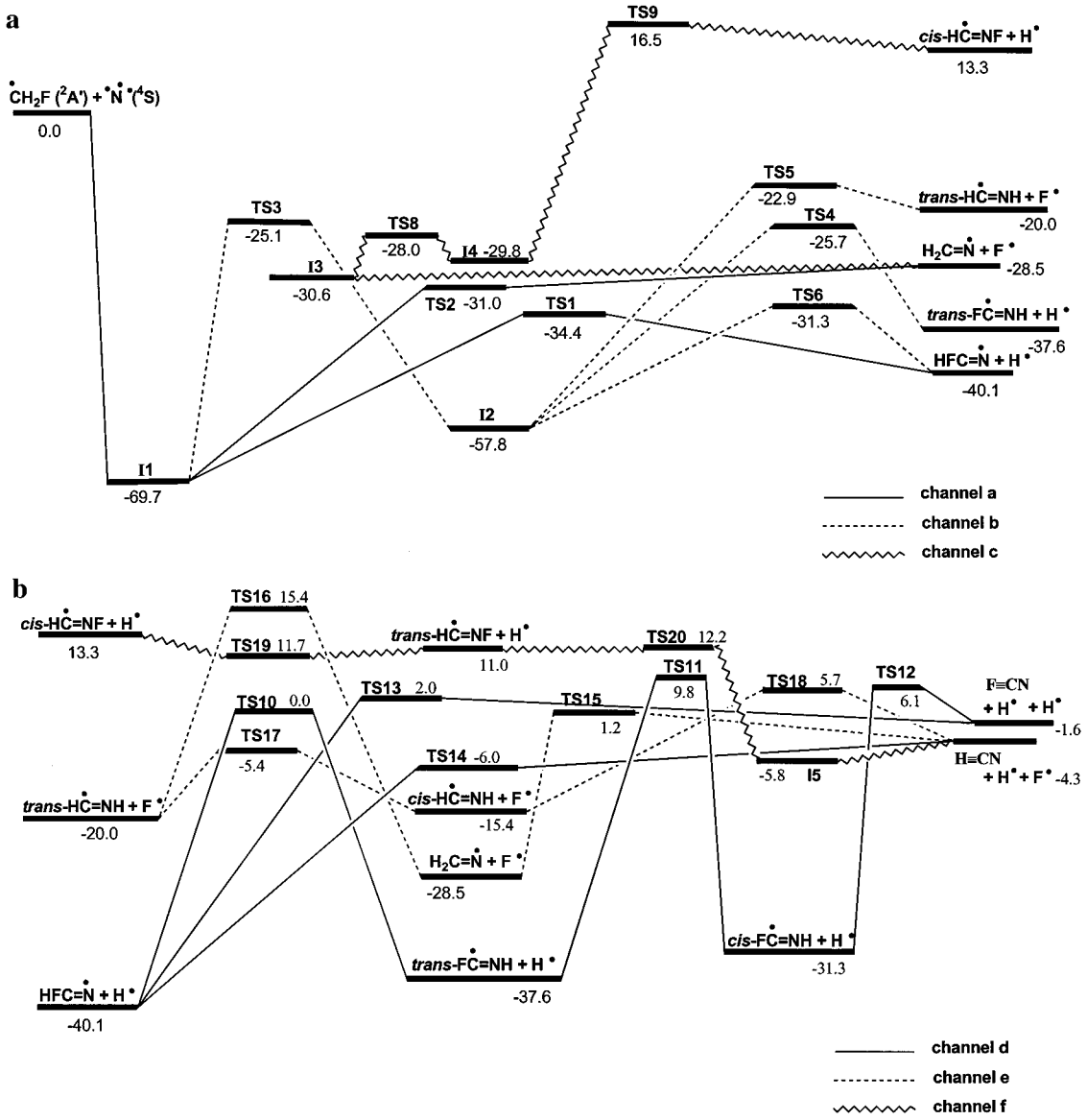

Figure 4. G2 reaction profiles (kcal/mol) for the formation of the primary products resulting from elimination of either hydrogen or fluorine atoms in the reaction N(^{4}S) + $CH_2F(^2A')$ and further evolution to give the final products FCN and HCN. See the text for the definition of the different channels (a−f).

reactants at different fixed C−N distances (from 1.4 to 5.6 Å), optimizing all other geometrical parameters. In both cases, a soft potential curve is obtained, thus confirming that the entrance of the reaction is a simple barrier-free path. Intermediate **I1** is rather stable at all levels of theory (nearly 70 kcal/mol below reactants at the G2 level; from now on, the G2 energies will be used in the discussion unless otherwise stated). We have also considered other interactions, such as those through the hydrogen and fluorine atoms, but all of them are much less favorable. Approaching of the reactants through the fluorine atom, that is, through an hypothetical intermediate which could be schematically represented as $^{\bullet}CH_2F\cdots N^{\bullet}$ (**I0**), takes place along a repulsive potential surface. Nevertheless, we have explored that possibility, and only a stationary point corresponding to that arrangement which lies quite high in energy, 61.7 kcal/mol above the reactants, was found. The characterization of this structure is problematic as a consequence of the small value of its lower frequency. MP2/cc-pVTZ frequency calculations showed that it is a minimum whereas at the MP2/6-31G(d,p) and MP2/cc-pVDZ levels it is a transition structure [at the MP2-(FULL)/6-31G(d) level, required to perform the G2 calculations, it is a minimum]. Furthermore, this species does not correlate exactly with the reactants, since in fact it can be represented as $^{\bullet}CH_2F\cdots N^{\bullet}$, that is, it corresponds to the triplet species obtained upon the interaction of $CH_2F(^2A')$ and N(^{2}D). The reasons for the notable endothermicity of the process leading to $^{\bullet}CH_2F\cdots N^{\bullet}$ (61.7 kcal/mol) can be found in the energy required to convert N(^{4}S) into N(^{2}D), which is 59.3 kcal/mol. Further evolution of this species has also been considered, but it involves even higher barriers. For example, the kinetic barrier associated with the formation of $H_2C^{\bullet}N^{\bullet}F$ (**I4**) is very high (**TS0**; 71.8 kcal/mol) as to play any relevant role in this reaction. The structures **I0**, **TS0**, and $^{\bullet}CH_2F\cdots N^{\bullet}$ have been incorporated into Scheme 1 for completeness, but the route $CH_2F(^2A') + N(^4S) \rightarrow CH_2F(^2A') + N(^2D) \rightarrow$ **I0** $\rightarrow$ **TS0** $\rightarrow$ **I4** was not considered in Figure 4 due to the highly unstable character of all the involved structures. Therefore, in what follows we shall limit the discussion only to the possible channels derived after formation of **I1**.

From inspection of Figures 4 and 5 and Scheme 1, once the intermediate **I1** is formed, several possibilities are opened. Channel a refers to all processes starting from **I1** that do not imply any isomerization. Those processes involving hydrogen

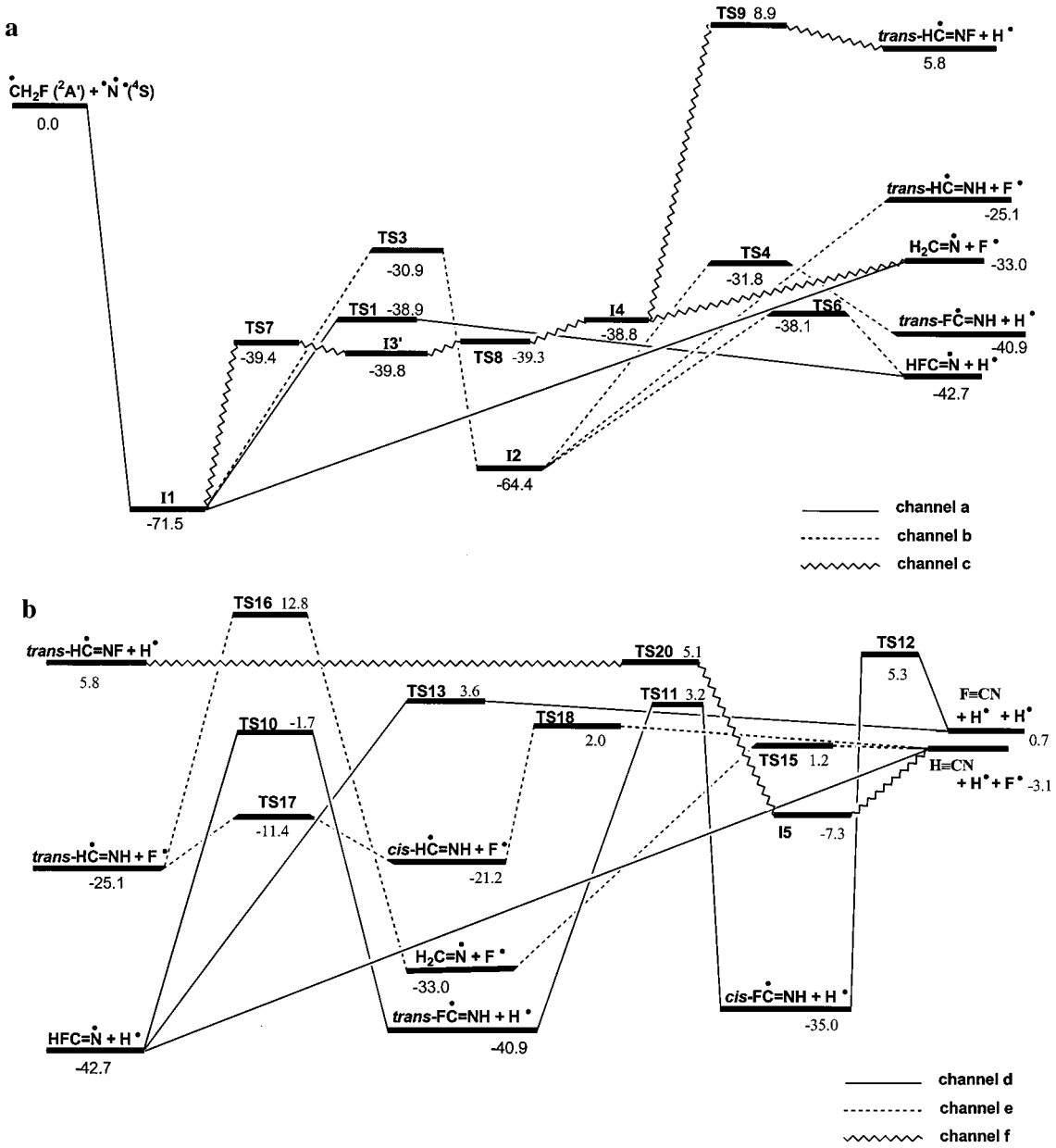

Figure 5. B3LYP/CBS reaction profiles (kcal/mol) for the formation of the primary products resulting from elimination of either hydrogen or fluorine atoms in the reaction $N(^4S) + CH_2F(^2A')$ and further evolution to give the final products FCN and HCN. The zero-point energy corrections as estimated at the B3LYP/cc-pVTZ level are included. See the text for the definition of the different channels (a−f).

migration and, therefore, taking place through the intermediate **I2** are generically denoted as channel b. Finally, channel c represents the different pathways leading to fluorine migration from carbon to nitrogen and, consequently, involving the intermediate **I4**.

Through channel a, **I1** ($^{\bullet\bullet}NCH_2F$) can undergo hydrogen abstraction, yielding one of the most stable products of the reaction, the $HFC{=}N^{\bullet}$ radical (−40.1 kcal/mol), through transition structure **TS1**, overcoming a barrier of 35.3 kcal/mol from **I1**. However, **TS1** lies well below the reactants (−34.4 kcal/mol). Another possibility for the evolution of **I1** is abstraction of the fluorine atom leading to a less exothermic product, $H_2C{=}N^{\bullet}$ (−28.5 kcal/mol). This is a direct process at the B3LYP level, as no transition structure for fluorine abstraction was found. However, the MP2 description of this process is different, since it involves a transition state for hydrogen abstraction (**TS2**). The slightly greater stability of **TS2** as compared with $H_2C{=}N^{\bullet} + F^{\bullet}$ shown in Figure 4 is an artifact arising from spin contamination. Of course, on the real MP2 PES (unprojected MP2 energies), the energy ordering of **TS2** and $H_2C{=}N^{\bullet} + F^{\bullet}$ is the correct one, namely, $^{\bullet\bullet}NCH_2F$ leads to $H_2C{=}N^{\bullet} + F^{\bullet}$, overcoming a barrier **TS2**. The energy values at the G2 level (see Table 1) show that **TS2** tends to disappear, becoming lower in energy than $H_2C{=}N^{\bullet} + F^{\bullet}$, thus suggesting fluorine abstraction to be a direct process in agreement with the B3LYP description.

The migration of a hydrogen atom from carbon to nitrogen in $^{\bullet\bullet}NCH_2F$ (channel b) proceeds through a transition structure very high in energy (**TS3**; 44.6 kcal/mol relative to **I1**) but still much lower in energy than the reactants (−25.1 kcal/mol). The resulting species is the quite stable diradical $HFC^{\bullet}N^{\bullet}H$ (−57.8 kcal/mol) denoted as **I2**. Such a diradical is the second most stable species on the triplet PES and might further transform into several final products. One of the possibilities is abstraction of the hydrogen atom bonded to carbon through **TS4** (with a high barrier of 32.1 kcal/mol) to give one of the most stable products, *trans*-$FC^{\bullet}{=}NH$ (−37.6 kcal/mol relative to reactants). A second pathway, corresponding to fluorine abstraction to give

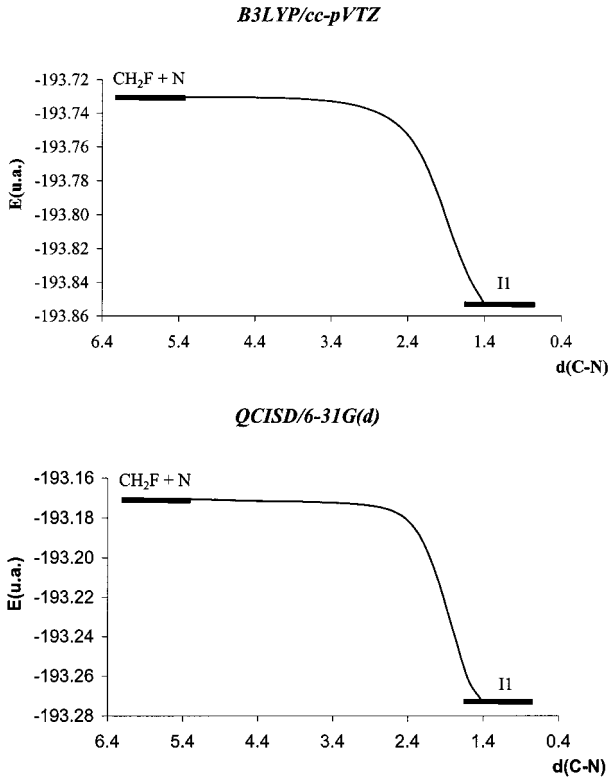

Figure 6. B3LYP/cc-PVTZ (top) and QCISD/6-31G(d) (bottom) profiles for the entrance channel of the N(^{4}S) + CH_2F (^{2}A′) reaction as a function of the C−N distance (in Å).

trans-HC•═NH, results in a much more unstable product (−20.0 kcal/mol) and even a higher barrier (**TS5**; 34.9 kcal/mol relative to **I2**). The **TS5** structure was not located at the B3LYP level. Finally, a third possibility is the elimination of the hydrogen atom bonded to nitrogen, which represents a second way of obtaining the HFC═N• radical through a high energetic barrier of 26.5 kcal/mol (**TS6**).

We shall finally comment the pathways involving isomerization of **I1** into **I4** through fluorine migration (channel c in Figure 4). This process is not easy to follow, since a gradual separation of the fluorine atom might involve weakly bound van der Waals structures whose characterization is not trivial. At the B3LYP level (see Figure 5), migration of fluorine atom toward nitrogen (**TS7**) first results in an intermediate, **I3′**, characterized by a long N−F distance and a wide C−N−F angle (see Figure 2). This intermediate is connected with the more stable structure **I4** through another transition state, **TS8**, which is also rather close in energy (spin contamination is responsible for the slightly greater stability of **TS8** with respect to **I4** shown in Figure 5). At the MP2 level, we were unsuccessful in finding any transition state similar to **TS7**. We should recall that in that region of the triplet PES the transition structure **TS2** was located at the MP2 level (see description of channel a above). Therefore, in the case of the MP2 surface, it seems that the first fluorine abstraction might take place (through **TS2**) without any significant barrier but its endothermicity. The fluorine atom may then recombine with H_2C═N• to form **I3** (different from the **I3′** structure located at the B3LYP level; see Figure 2 and Figure 5), which transforms into **I4** through **TS8** (see Figure 4). Although this description of the process is certainly different from that in the case of the B3LYP PES, there is in fact little difference from a practical point of view (compare the B3LYP **I1** → **TS7** → **I3′** → **TS8** → **I4** and MP2 **I1** → **TS2** → H_2C═N• + F• → **I3** → **TS8** → **I4** routes in Scheme 1; while the B3LYP **I3′** structure is directly connected with **I1**, the MP2 **I3** structure is not).

H_2C•N•F (**I4**) may further evolve through hydrogen abstraction to the less stable product, *cis*-H•C═NF (13.3 kcal/mol above the reactants), involving also a high barrier (**TS9**, 46.3 kcal/mol). It should be mentioned that at the B3LYP level the *trans*-H•C═NF isomer is obtained instead of the *cis*-H•C═NF isomer. At this latter level, **I4** may suffer fluorine elimination to give H_2C═N• + F•, through a process which proceeds without any barrier (see Figure 5). As mentioned above, the same process at the MP2 level involves a quite small barrier (**TS8**; 1.8 kcal/mol above **I4**) and a weakly bound complex (**I3**).

From the energy results collected in Table 1 and Figures 4 and 5, it is clear that there are two products which are thermodynamically favored, namely, HFC═N• + H• and *trans*-FC•═NH + H•. In these two products, the fluorine atom is retained bonded to carbon, whereas a hydrogen atom is eliminated. Those products corresponding to abstraction of fluorine, *trans*-HC•═NH + F• and H_2C═N• + F•, are still exothermic, but they are about 15−20 kcal/mol higher than the most favored ones. Finally, production of *cis*-HC•═NF + H•, with fluorine bonded to the nitrogen atom, is endothermic and consequently clearly disfavored. Calculations [G2, B3LYP/CBS and CCSD(T) levels] suggest that the thermodynamically favored product is HFC═N• (by 1.8−3.3 kcal/mol), although MP2/CBS slightly favors *trans*-FC•═NH. All the theoretical levels agree, in general, that the production of HFC═N• + H• should be kinetically favored, since **TS1** lies below both **TS3** (about 8.1−9.3 kcal/mol, depending on the level of calculation) and **TS2** (about 3.4−9.5 kcal/mol). **TS8** in channel c results slightly lower in energy at the B3LYP/CBS level (by only 0.4 kcal/mol; see Figure 5), but it is clearly higher in energy at the CCSD(T)//B3LYP level.

To lend further support to our conclusions, we have carried out additional calculations for the more important channels, namely, formation of HFCN, *trans*-FCNH, and H_2CN. To this end, we have carried out QCISD/6-31G(d,p) optimizations of the different products, intermediates, and transition states involved in those channels, followed by single-point calculations to refine the electronic energy at the QCISD(T)/cc-pVTZ level. QCISD[16] stands for quadratic configuration interaction with single and double substitutions, whereas (T) means a perturbative treatment of triple substitutions. QCISD should be less sensible to spin contamination than MP2, and although strictly speaking it is a single-reference method, QCISD should also perform better if the system under study has a moderate multiconfigurational character.[36] In general, as can be seen in Table 1, the QCISD/6-31G(d,p) results are not far from the MP2 ones obtained with the same basis set, whereas the QCISD(T)/cc-pVTZ relative energies are in most cases halfway between the MP2 ones and the G2 values. Nevertheless, it is interesting to point out that extrapolated MP2/CBS relative energies are in general much closer to the reference G2 values than the QCISD(T)//QCISD ones.

Another interesting question is the validity of the G2 method for predicting relative energies for transition states, since there is no calibration of G2 for predicting energy barriers. For that purpose, we have carried out G3[37] calculations for selected transition states (those whose relative energy ordering is important for the conclusions of the work), namely, TS1, TS2, TS3, and TS8. The results are also shown (in parentheses) in Table 1. As can be seen the G3 results, which are highly reliable for TS's, virtually match the G2 ones, the largest discrepancy being just 0.7 kcal/mol. Most important, the relative energy

ordering of these transition states is exactly the same obtained at the G2 level, giving further support to the validity of estimated G2 reaction barriers for the reaction under study.

It should be mentioned that the possible formation of HC≡N + FH or FC≡N + H_2 has not been considered in Scheme 1 and Figures 4 and 5 since it would imply one of the molecules to be in a triplet state, thus giving rise to rather endothermic channels. However, we have considered the possibility of further evolution of the primarily formed products. Thus, in Figures 4 and 5 (as well as in Scheme 1), the energy profiles for the possible evolution of HFC═N$^{\bullet}$ (channel d), *trans*-HC$^{\bullet}$═NH (channel e), and *cis*-HC$^{\bullet}$═NF (channel f) are represented. Subsequent fragmentation processes which can take place through a second elimination of either hydrogen or fluorine atoms are also shown. It should be pointed out that we have added to the energy of the different transition structures in Figures 4b and 5b and Table 1 the energy of the previously eliminated fragment. In that way, we are evaluating their energies relative to the initial reactants, and therefore, a direct comparison with the first part of Figures 4 and 5 is feasible.

The two most stable initial products of the N(^{4}S) + CH_2F-(^{2}A′) reaction, namely, HFC═N$^{\bullet}$ and *trans*-FC$^{\bullet}$═NH, may be connected through a transition state (**TS10**) which is nearly isoenergetic with the reactants and therefore implies a considerable kinetic barrier (about 40 kcal/mol). Further isomerization of *trans*-FC$^{\bullet}$═NH into *cis*-FC$^{\bullet}$═NH involves a transition structure (**TS11**) that lies 9.8 kcal/mol above the reactants. Fragmentation of a second hydrogen atom from *cis*-FC$^{\bullet}$═NH is also subject to a considerable barrier (**TS12**; about 40 kcal/mol). Finally, fragmentation of HFC═N$^{\bullet}$, through elimination of a second hydrogen atom (**TS13**), involves a high barrier (about 42 kcal/mol), whereas the most favorable process for HFC═N$^{\bullet}$ seems to be fragmentation into HC≡N + F$^{\bullet}$, since the corresponding transition structure lies slightly below the reactants (**TS14**; −6 kcal/mol). At the B3LYP level, fragmentation of fluorine is a direct process, and therefore, **TS14** is not present on the corresponding PES. Nevertheless, this is not an important difference, since **TS14** lies only slightly higher in energy (about 3 kcal/mol) than the final products at the MP2/CBS level (at the G2 level, it is predicted to be even lower in energy than HC≡N + H$^{\bullet}$ + F$^{\bullet}$).

The next primary product in stability order is H_2C═N$^{\bullet}$. Elimination of a hydrogen atom results in HC≡N, a process involving a transition structure (**TS15**) which lies somewhat higher in energy than reactants (1.2 kcal/mol). Isomerization between H_2C═N$^{\bullet}$ and *trans*-HC$^{\bullet}$═NH is subject to a high barrier (**TS16**; 15.4 kcal/mol above reactants), and therefore, it is quite unlikely to occur. As expected, isomerization between the trans and cis isomers of HC$^{\bullet}$═NH involves a much smaller barrier (**TS17**; about 15 kcal/mol). Nevertheless, the primary product, *trans*-HC$^{\bullet}$═NH, is more stable than the cis isomer. Further fragmentation of *cis*-HC$^{\bullet}$═NH produces again HC≡N through a transition state (**TS18**) which implies a relatively high barrier of about 21 kcal/mol.

Finally, both isomers of HC$^{\bullet}$═NF as well as the transition structures for their isomerization (**TS19**; not present on the B3LYP PES) and for fluorine elimination (**TS20**), the latter passing through a weakly bound structure HC≡N···F$^{\bullet}$ (**I5**) to give HC≡N, are quite close in energy. All these species are much higher in energy than the reactants (more than 10 kcal/mol at the G2 level in all cases).

The main conclusion from Figures 4b and 5b is that further evolution of the primary products of the N(^{4}S) + CH_2F(^{2}A′) reaction is quite unlikely, since it is not favored neither thermodynamically nor kinetically. In particular, further fragmentation to produce either FC≡N or HC≡N has a low exothermicity and is subject in all cases to high energy barriers.

We may compare our results for the N(^{4}S) + CH_2F reaction with those obtained for the reaction of nitrogen atoms with methyl radicals. In the case of the N(^{4}S) + CH_3 reaction, both experimental[3] and theoretical[1] works agree in that the major product is H_2CN+H. The theoretical study by Gonzalez and Schlegel suggests that the reaction proceeds through the direct formation of an intermediate, similar to **I1**, which lies about 62 kcal/mol below the reactants at the PMP4 level (our G2 value for **I1** is −69.7 kcal/mol). Therefore, there is a certain coincidence in the basic mechanistic aspects (addition−elimination reaction; relatively stable intermediate), as well as in the predicted main product, HFCN + H, which implies elimination of a hydrogen atom from the intermediate. Nevertheless, it is interesting to point out the preference for a product incorporating the fluorine atom in the case of the reaction with CH_2F, which is also reflected in the fact that the second most favorable product is *trans*-FCNH + H, instead of H_2CN + F.

Conclusions

A theoretical study of the triplet potential energy surface for the reaction of ground-state nitrogen atoms with the fluorinated methyl radical has been carried out. The reaction proceeds via a typical addition−elimination mechanism, where initially an intermediate ($^{\bullet\bullet}$$NCH_2F$), which is relatively stable, is formed upon interaction of nitrogen with the radical through the carbon atom. Bearing in mind the energies of all the species appearing in Scheme 1, it is clear that there are two preferred products from the thermodynamic viewpoint which imply elimination of a hydrogen atom, *trans*-FC$^{\bullet}$═NH and HFC═N$^{\bullet}$, the latter one being slightly more stable. Other possible products, such as H_2C═N$^{\bullet}$ and *trans*-HC$^{\bullet}$═NH, are also exothermic but less stable, whereas *cis*-HC$^{\bullet}$═NF is even clearly endothermic. From the kinetic viewpoint, both *trans*-FC$^{\bullet}$═NH and HFC═N$^{\bullet}$ are obtained through pathways involving transition structures which clearly lie below the reactants. However, HFC═N$^{\bullet}$ should be the preferred product since the barrier relative to the intermediate $^{\bullet\bullet}$$NCH_2F$ is much smaller than the corresponding barrier involved in the production of *trans*-FC$^{\bullet}$═NH. Our study also reveals that further evolution of the primary products, via subsequent elimination of hydrogen or fluorine atoms or via rearrangement into other isomeric species, is not likely, since all these processes are much less exothermic and involve considerable kinetic barriers.

From the methodological viewpoint, the geometries computed with MP2 and B3LYP methods agree within 0.02 Å (bond distances) and 3° (angles). Concerning the performance of the different methods employed in the present work to estimate the energies of the structures involved, it seems that MP2/CBS might be a reasonable compromise between quality of results and computational cost, since it usually provides relative energies in good agreement with G2. On the other hand, B3LYP consistently provides energy values appreciably lower than those of G2, especially for some transition structures. Nevertheless, the relative ordering of the different species is virtually the same as that provided by MP2/CBS or G2.

Acknowledgment. This research has been supported by the Ministerio de Educación y Cultura of Spain (DGICYT, Grant PB97-0399-C03) and by the Junta de Castilla y León (Grant VA 18/00B).

References and Notes

(1) Gonzalez, C.; Schlegel, H. B. *J. Am. Chem. Soc.* **1992**, *114*, 9118.
(2) Marston, G.; Nesbitt, F. L.; Nava, D. F.; Payne, W. A.; Stief, L. J. *J. Phys. Chem.* **1989**, *93*, 5769.
(3) Marston, G.; Nesbitt, F. L.; Stief, L. J. *J. Chem. Phys.* **1989**, *91*, 3483.
(4) Nejad, L. A. M.; Millar, T. J. *Mon. Not. R. Astron. Soc.* **1988**, *230*, 79.
(5) Yung, Y. L.; Allen, M.; Pinto, J. P. *Astrophys. J. Suppl. Ser. Phys.* **1984**, *55*, 465.
(6) Glarborg, P.; Miller, J. A.; Kee, R. J. *Combust. Flame* **1986**, *65*, 177.
(7) Safrany, D. R. *Prog. React. Kinet.* **1971**, *6*, 129.
(8) Jeoung, S. C.; Choo, K. Y.; Benson, S. W. *J. Phys. Chem.* **1991**, *95*, 7282.
(9) Tsai, C.; Belanger, S. M.; Kim, J. T.; Lord, J. R.; Mcfadden, D. L. *J. Phys. Chem.* **1989**, *93*, 1916.
(10) Seetula, J. A.; Slagle, I. R.; Gutman, D.; Senkan, S. M.; Itoh, S. *Chem. Phys. Lett.* **1996**, *252*, 299.
(11) Seetula, J. A.; Slagle, I. R. *Chem. Phys. Lett.* **1997**, *277*, 381.
(12) Wang, B.; Hou, H.; Gu, Y. *J. Phys. Chem. A* **1999**, *103*, 2060.
(13) Wang, B.; Hou, H.; Gu, Y. *J. Phys. Chem. A* **1999**, *103*, 5075.
(14) Wang, B.; Hou, H.; Gu, Y. *Chem. Phys. Lett.* **1999**, *304*, 278.
(15) Wang, B.; Hou, H.; Gu, Y. *Chem. Phys.* **1999**, *247*, 201.
(16) Hehre, W. J.; Radom, L.; Schleyer, P. v. R.; Pople, J. A. *Ab initio Molecular Orbital Theory*; Wiley: New York, 1986.
(17) Bartlett, R. J.; Stanton, J. F. *Reviews in Computational Chemistry*; VCH: New York, 1994; Vol. 5.
(18) Becke, A. D. *J. Chem. Phys.* **1992**, *97*, 9173.
(19) Lee, C.; Yang, W.; Parr, R. G. *Phys. Rev. B* **1988**, *37*, 785.
(20) Dunning, T. H., Jr. *J. Chem. Phys.* **1989**, *96*, 1007.
(21) Feller, D.; Sordo, J. A. *J. Chem. Phys.* **2000**, *112*, 5604.
(22) Feller, D.; Sordo, J. A. *J. Chem. Phys.* **2000**, *113*, 485.
(23) Sordo, J. A. *J. Chem. Phys.* **2001**, *114*, 1974.
(24) Dunning, T. H., Jr. *J. Phys. Chem.* **2000**, *104*, 9062.
(25) Lynch, B. J.; Truhlar, D. G. *J. Phys. Chem. A* **2001**, *105*, 2936.
(26) Curtiss, L. A.; Raghavachari, K.; Trucks, G. W.; Pople, J. A. *J. Chem. Phys.* **1991**, *94*, 7221.
(27) Woon, D. E.; Dunning, T. H., Jr. *J. Chem. Phys.* **1994**, *101*, 8877.
(28) Feller, D.; Peterson, K. A. *J. Chem. Phys.* **1998**, *108*, 154.
(29) Schlegel, H. B. *J. Chem. Phys.* **1986**, *84*, 4530.
(30) Jensen, F. *Introduction to Computational Chemistry*; Wiley: Chichester, U.K., 1999.
(31) Stanton, J. F. *J. Chem. Phys.* **1994**, *101*, 371.
(32) Gonzalez, C.; Schlegel, H. B. *J. Chem. Phys.* **1989**, *90*, 2154.
(33) Gonzalez, C.; Schlegel, H. B. *J. Chem. Phys.* **1990**, *94*, 5523.
(34) Frisch, M. J.; Trucks, G. W.; Schlegel, H. B.; Scuseria, G. E.; Robb, M. A.; Cheeseman, J. R.; Zakrzewski, V. G.; Montgomery, J. A., Jr.; Stratmann, R. E.; Burant, J. C.; Dapprich, S.; Millan, J. M.; Daniels, A. D.; Kudin, K. N.; Strain, M. C.; Farkas, O.; Tomasi, J.; Barone, V.; Cossi, M.; Cammi, R.; Mennucci, B.; Pomelly, C.; Adamo, C.; Clifford, S.; Ochterski, J.; Petersson, G. A.; Ayala, P. Y.; Cui, Q.; Morokuma, K.; Malick, D. K.; Rabuck, A. D.; Raghavachari, K.; Foresman, J. B.; Cioslowski, J.; Ortiz, J. V.; Baboul, A. G.; Stefanov, B. B.; Liu, G.; Liashenko, A.; Piskorz, P.; Komaromi, I.; Gomperts, R.; Martin, R. L.; Fox, D. J.; Keith, T.; Al-Laham, M. A.; Peng, C. Y.; Nanayakkara, A.; Gonzalez, C.; Challacombe, M.; Gill, P. M. W.; Johnson, B.; Chen, W.; Wong, M. W.; Andres, J. L.; Head-Gordon, M.; Replogle, E. S.; Pople, J. A. *Gaussian 98*; Gaussian Inc.: Pittsburgh, PA, 1998.
(35) Barrientos, C.; Redondo, P.; Largo, A. *J. Phys. Chem. A* **2000**, *104*, 11541.
(36) Bally, T.; Borden, W. T. In *Reviews in Computational Chemistry*; Lipkowitz, K. B., Boyd, D. B. Eds.; Wiley-VCH: New York, 1999; Vol. 13.
(37) Curtiss, L. A.; Raghavachari, K.; Redfern, P. C.; Rassolov, V.; Pople, J. A. *J. Chem. Phys.* **1998**, *109*, 7764.